Journal Pre-proofs

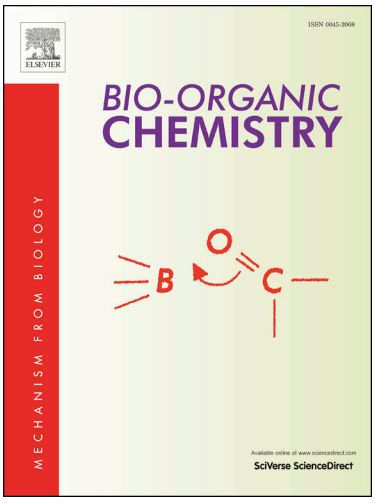

Identification of a potent heme oxygenase-2 (HO-2) inhibitor by targeting the secondary hydrophobic pocket of the HO-2 western region

Giuseppe Floresta, Antonino N. Fallica, Giuseppe Romeo, Valeria Sorrenti, Loredana Salerno, Antonio Rescifina, Valeria Pittalà

PII: S0045-2068(20)31608-4
DOI: https://doi.org/10.1016/j.bioorg.2020.104310
Reference: YBIOO 104310

To appear in: *Bioorganic Chemistry*

Received Date: 16 July 2020
Revised Date: 15 September 2020
Accepted Date: 20 September 2020

Please cite this article as: G. Floresta, A.N. Fallica, G. Romeo, V. Sorrenti, L. Salerno, A. Rescifina, V. Pittalà, Identification of a potent heme oxygenase-2 (HO-2) inhibitor by targeting the secondary hydrophobic pocket of the HO-2 western region, *Bioorganic Chemistry* (2020), doi: https://doi.org/10.1016/j.bioorg.2020.104310

Identification of a potent heme oxygenase-2 (HO-2) inhibitor by targeting the secondary hydrophobic pocket of the HO-2 western region

Giuseppe Floresta [a, b], Antonino N. Fallica [a], Giuseppe Romeo [a], Valeria Sorrenti [a], Loredana Salerno [a], Antonio Rescifina [a], Valeria Pittalà [a,*]

[a] Department of Drug Sciences, University of Catania, V.le A. Doria 6, 95125 – Catania, Italy

[b] Department of Analytics, Environmental & Forensics, King's College London, Stamford Street, London SE1 9NH, UK

Corresponding author:

*Valeria Pittalà vpittala@unict.it

Graphical abstract

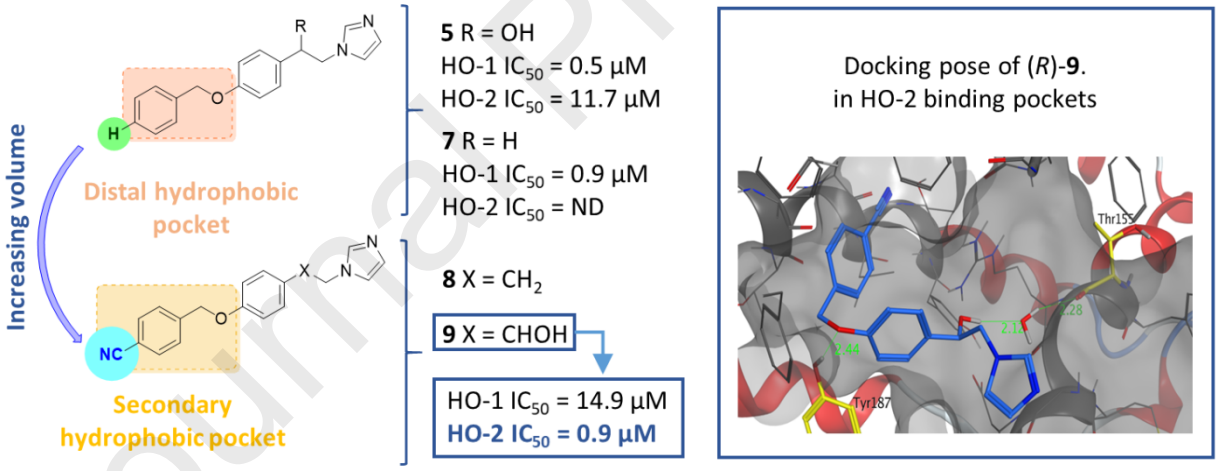

Highlights

- HO-2 selective inhibitors have been designed
- Selectivity switch from HO-1 to HO-2 was obtained by increasing the volume of the molecules
- Docking studies rationalized the obtained results
- The presence of a Tyr187 residue in HO-2 accounts for the binding pose of **9**

Keywords: Heme oxygenase-2, heme oxygenase-1, imidazole derivatives, structure-activity relationships, western region, azalanstat.

Abstract

The enzymatic family of heme oxygenase (HO) is accountable for heme breakdown. Among the two isoforms characterized to date, HO-2 is poorly investigated due to the lack of potent HO-2 chemical modulators and the greater attentiveness towards HO-1 isoform. In the present paper, we report the rational design and synthesis of HO-2 inhibitors achieved by modulating the volume of known HO-1 inhibitors. The inhibition preference has been moved from HO-1 to HO-2 by merely increasing the volume of the substituent in the western region of the inhibitors. Docking studies demonstrated that new derivatives soak differently in the two binding pockets, probably due to the presence of a Tyr187 residue in HO-2. These findings could be useful for the design of new selective HO-2 compounds.

1. Introduction

Endogenous enzymes in control of heme breakdown are known as heme oxygenases (HOs). These enzymes exert cytoprotective roles in organs and are responsible for degrading senescent red-blood cells through the removal of the pro-inflammatory heme and the production of protecting by-products such as carbon monoxide (CO) and bilirubin [1]. This group of enzymes includes two well-characterized isoforms, heme oxygenase-1 (HO-1) and heme oxygenase-2 (HO-2), differing for distribution and expression level under different conditions. HO-1 is highly represented only in limited areas such as the liver and spleen, whereas HO-2 is widely distributed among different endogenous areas with a prevalence in the brain, testes, endothelial and smooth muscle cells, myenteric gut plexus, nephrons, and liver [2]. However, while HO-2 distribution remains unchanged regardless of the endogenous oxidative stress status, HO-1 undergoes an overexpression process, controlled by the transcription factor nuclear factor erythroid 2-related factor-2 (Nrf2), with

consequent increment in districts where cellular stress must be reduced [1, 3-5]. For such reason, HO-1 received considerable attention in recent years, and the use of HO-1 inducers are advantageous in various oxidative stresses dependent syndromes [6-12].

Nonetheless, an increasing amount of literature recently suggests that HO-1 might play its part in tumor initiation. HO-1 expression is frequently heightened in cancer tissues promoting atypical cellular growth and metastasis onset in different types of cancer and eventually leads to reduced chances of survival [13, 14]. Also, HO-1 levels could be further boosted when those tissues are exposed to different types of tumor treatment, such as radio-, chemo-, or photodynamic [15-18]. It can powerfully improve the growth and spread of cancers suggesting that the role of HO-1 in heme metabolism makes it an essential mediator to protective effects not only towards healthy cells but also towards the cancerous ones. Previous studies demonstrated the involvement of HO-1 in different tumors, including leukemia, glioblastoma, neuroblastoma, prostate, breast, lung, head, and neck cancers [14, 19-21]. Because of this, HO-1 inhibition might reduce aberrant cellular proliferation, tumor invasion, and progression [22-26].

Dissimilar to HO-1 inhibitors/activators, the possible beneficial applications of HO-2 ligands have not been systematically investigated so far [27]. Moreover, the functional role of HO-2 is still elusive, mostly owing to the absence of highly potent HO-2 chemical modulators and the higher interest towards HO-1 isoform. HO-2 physiological roles have been studied mostly in organs such as the liver, testis, and brain, where this isoform is expressed constitutively and is more abundant [2, 28]. For instance, in testis, HO-2 seems to take part in male reproduction and in the modulation of the ejaculatory activity. The role of HO-2 in the brain is still puzzling, and it is the subject of numerous investigations due to its favorable involvement in neuroprotection and brain injuries [29]. Although increasing knowledge has been gained over the past decade to unravel the physiological role of HO-2, its full potential as a druggable target remains to be elucidated. Therefore, the development of selective and potent HO-2 inhibitors and/or activators is required as pharmacological tools to gain knowledge in the field.

Historically, heme analogs (metalloporphyrins, MPs) lead the research to the development of HO inhibitors; however, their off-target effects limited their translation into the clinic. Therefore, the attention was devoted to azalanstat (Figure 1, compound **1**) that served as a lead compound for the development of selective non-competitive HO-1 and HO-2 inhibitors.

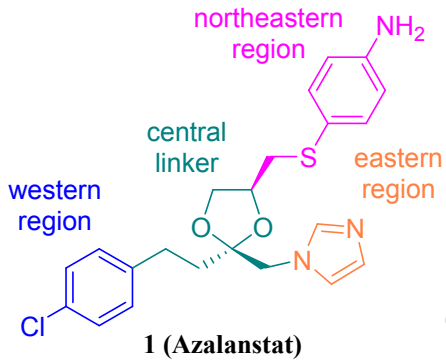

1 (Azalanstat)

IC_{50} HO-1 = 5.3 μM
IC_{50} HO-2 = 24.4 μM

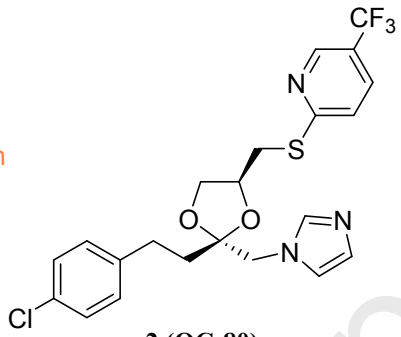

2 (QC-80)

IC_{50} HO-1 = 2.1 μM
IC_{50} HO-2 = 16 μM

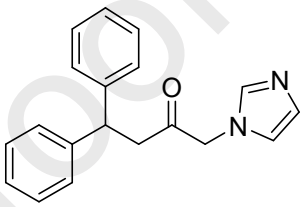

3 (QC-308)

IC_{50} HO-1 = 0.27 μM
IC_{50} HO-2 = 0.46 μM

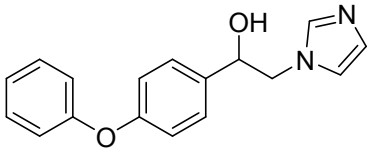

4

IC_{50} HO-1 = 0.9 μM
IC_{50} HO-2 = 10.5 μM

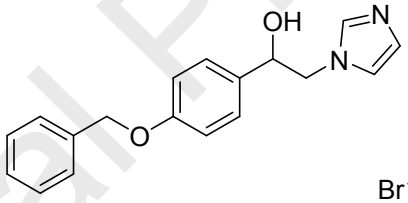

5

IC_{50} HO-1 = 0.50 μM
IC_{50} HO-2 = 11.7 μM

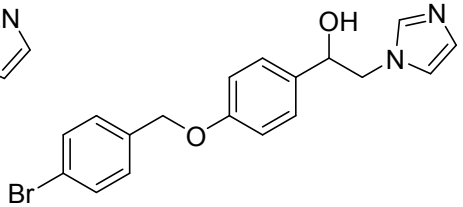

6

IC_{50} HO-1 = 0.9 μM
IC_{50} HO-2 > 100 μM

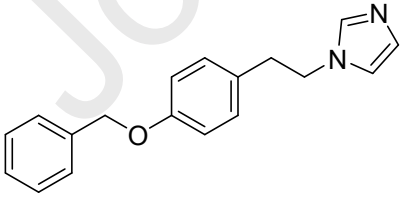

7

IC_{50} HO-1 = 0.9 μM
IC_{50} HO-2 = ND

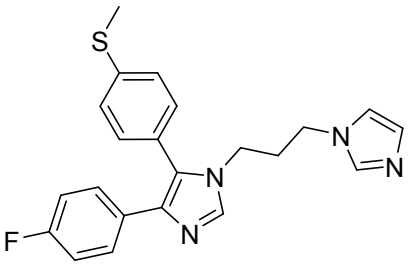

SLV-11199

IC_{50} HO-1 = 2.23 μM
IC_{50} HO-2 = 1.07 μM

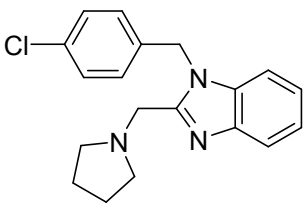

Clemizole

IC_{50} HO-1 > 100 μM
IC_{50} HO-2 = 3.4 μM

Figure 1. Chemical structure of lead compounds, azalanstat, QC-80, QC-308, and other representatives HO selective and non-selective inhibitors.

More than fifteen years of studies on the structure-activity relationships (SARs) on azalanstat focused on the development of selective HO-1 inhibitors allowed the identification of the main key features for HO inhibition, as confirmed by crystallization studies of HO-1 inhibitors complexed with the enzyme [29-31]. Briefly, four main regions (northeastern, eastern, central, and western) can be recognized in the chemical structure of azalanstat corresponding to four primary areas of interactions inside the HO binding pocket. The northeastern area is not mandatory for HO-1 inhibition, and it is often removed. The eastern region is the most preserved portion of the molecule since it permits the binding to the Fe^{2+} of heme. An unsubstituted imidazole provides the best results in term of potency; limited modifications are tolerated in this area, and the majority of them leads to loss of inhibition potency. The central part can be subjected to various modifications regarding the length and the presence of different functional groups/heteroatoms, allowing the optimization of the inhibitory activity. The western region offers a right area for the modulation of activity and selectivity. The type, volume, and nature of the substituents present in this area (large hydrophobic groups seem to be preferred) can additionally stabilize the heme-binding. Substituents in this area interact with the distal hydrophobic pocket of HO. Of interest is the high flexibility of this pocket and the consequent capability to receive moieties of different sizes. Also, crystallization studies on QC-80 and QC-308 (Figure 1, compounds **2** and **3**, respectively) brought to light the presence of a secondary small hydrophobic pocket in the western region [32, 33]. Interactions with this secondary pocket seem to enhance binding potency towards both HO-1 and HO-2 isoforms.

Over the past decade, our research group has been continuously involved in the rational design of selective inhibitors directed towards the two HO isoforms using azole-based scaffolds [23, 25, 34-37]. To this extent, we built a free-internet accessible database bringing together all the HO inhibitors published so far, whose analysis empowered the design of potent selective and non-selective HO-1 inhibitors such as compounds **4-7** (Figure 1) [37-39]. Recently, Mucha and coworkers reported the development and characterization of a novel non-selective HO inhibitor, SLV-11199 (Figure 1), with

anticancer effects on human pancreatic (PANC-1) and prostate (DU-145) cancer cell lines [40]. The chemical structure of this novel compound presents the usual imidazole ring in the eastern region; however, an additional 1,4,5-trisubstituted imidazole ring is present in the central region, allowing a more rigid structure and an additional hydrogen bond with the Arg136 sidechain in the catalytic pocket of the enzyme. This additional interaction, together with the binding mode similar to that of QC-308, explains the potent inhibitory activity of SLV-11199 towards both HO isoforms, even if selectivity issues remain. Pushed by these results, the activity of SLV-11199 was evaluated in hereditary leiomyomatosis and renal cell carcinoma (HLRCC), a cancer cell line characterized by deficiency in the fumarate hydratase (FH) gene. Genetic or pharmacological inhibition of HO-1 with SLV-11199 in FH deficient cell lines leads to synthetic lethality [41]. Fewer studies have been specifically conducted in search of selective HO-2 inhibitors, which lead to the identification of the highly selective clemizole (Figure 1), possessing a benzimidazole scaffold [42]. Structure-activity relationships studies on clemizole have been performed by changing the substituents at N-1 position. The novel derivatives showed to possess similar or slight better potencies against HO-2, and their development represented the first attempt for the search of selective HO-2 inhibitors.

The aim of the present study is the rational design and synthesis of a small series of derivatives oriented towards HO-2 selective inhibition. To this extent, we maintained fixed the imidazole ring and the length of the spacer, rationally modifying the nature of the spacer and the volume of the western region in order to switch both selectivity and potency towards HO-2.

2. Results and Discussion

2.1. Rationale design

As already pointed out in our previous work, the selectivity between the two different isoforms can be triggered by the volume of the molecules and so the design of a novel inhibitor can be tuned exploiting these observations [37]. In fact, even if the binding pockets of the two proteins are relatively flexible, the four most selective, and also potent HO-1 inhibitors, retrieved by the heme-

oxygenase database (HemeOxDB2, HemeOxDB16, HemeOxDB18, HemeOxDB20; http://www.researchdsf.unict.it/hemeoxdb/) possess a mean Van der Waals volume of 274.34 Å^3 with an interval of 239.00–302.87 Å^3; differently, potent and selective HO-2 inhibitors (HemeOxDB187, HemeOxDB200, HemeOxDB202, and HemeOxDB286) have a mean volume of 284.10 Å^3 with an interval of 274.37–306.75 Å^3 [37-39]. These observations lead us to think that the volume of the ligands is an essential factor influencing the selectivity, considering as a rule of thumb that the larger the cavity of the isoform, the greater the volume of the ligand to achieve the best binding potency and selectivity. This empirical rule was already successful for the design of novel HO-1 inhibitors [37] (*i.e.*, smaller molecules for selective and potent HO-1 compounds). This work aimed to apply the same rule for the design of novel HO-2 selective compounds (*i.e.*, bigger molecules for selective and potent HO-2 compounds); moreover, the bigger ligand should be easily accommodated in the secondary hydrophobic pocket of the HO-2 western region.

To actively validate this hypothesis, we designed the HO-2 inhibitors starting from two molecules with high HO-1 inhibition activity but not with high selectivity. So, we simply increased the volume of the compounds **5** and **7** adding them a cyano group, as shown in Table 1. In both cases, the selected cyano group added about 20 Å^3 to the final volume of the molecules (Table 1, *i.e.*, increasing the volume size and so theoretically moving the selectivity from HO-1 to HO-2); moreover, the position 4 of the ring system was selected to explore possible interactions with the bottom of the secondary hydrophobic pocket of the HO-2 western region (Figure 2). The cyano group has also been selected because able to be placed deeper in the HO-2 cavity. In fact, despite molecule **9** has a bigger but similar volume than the bromo-derivative **6** (336.32 Å *vs*. 334.46 Å), the cyano group led the molecule to reach the bottom of the secondary hydrophobic pocket of the HO-2 western region, differently to compound **6** (Figure 1). The measured distances between the nitrogen of molecule **9**, the bromine of **6**, and the respective benzylic CH_2 are 6.88 and 6.10 Å, respectively (Figure 3).

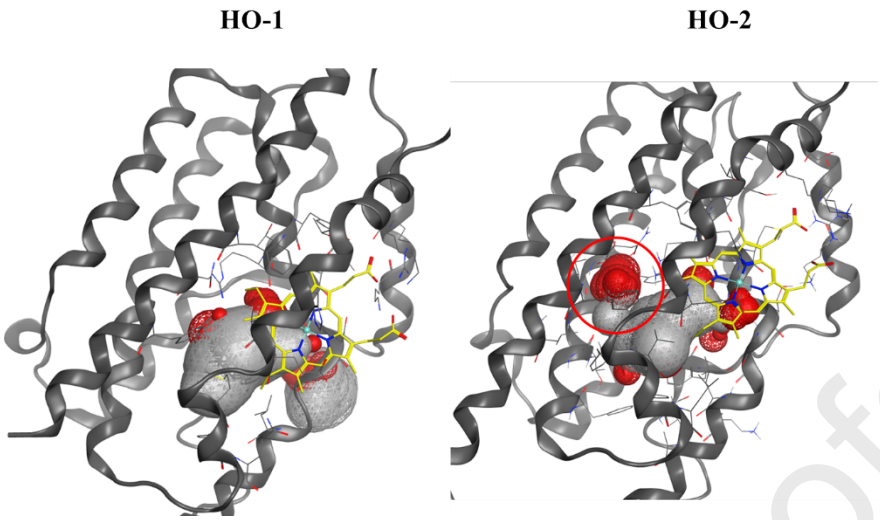

Figure 2. Left. HO-1 binding pocket (PDB ID: 2DY5). Right, HO-2 binding pocket (PDB ID: 2QPP), the secondary hydrophobic pocket of the HO-2 western region, is circled in red.

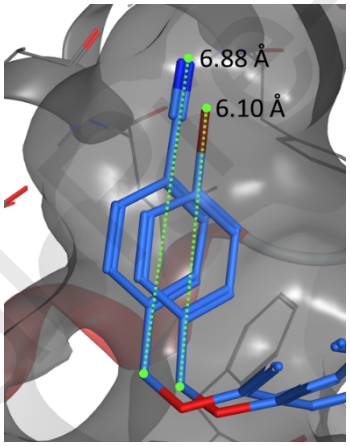

Figure 3. Distances between the nitrogen of molecule **9**, the bromine of molecule **6**, and the respectively benzylic CH_2 inside the secondary hydrophobic pocket of the HO-2 western region.

2.2. Chemistry

The general synthetic pathway to the new compounds is depicted in Scheme 1. Compound **8** was prepared in two steps as follows: the reaction between 4-(bromomethyl)benzonitrile and 4-(2-bromoethyl)phenol in acetone afforded the bromide derivative **10**. This intermediate was converted to the final compound **8** through a nucleophilic displacement using an excess of imidazole in the presence of TEA and TBAB, using dry CH_3CN as solvent.

The synthesis of compounds **13** and **9** passes through the formation of the intermediate **11** that was prepared by reaction of 1-(4-hydroxyphenyl)ethanone with 4-(bromomethyl)benzonitrile, as reported in Scheme 1. The 1-substituted bromomethyl ketone **12** was obtained by bromination, in the glacial acetic acid, of the corresponding ketone **11**. The latter has been used without purification to synthesize compound **13**, through a nucleophilic displacement using an excess of imidazole in the presence of K_2CO_3. The obtained ketone **13** was then reduced with $NaBH_4$ to the final compound **9**.

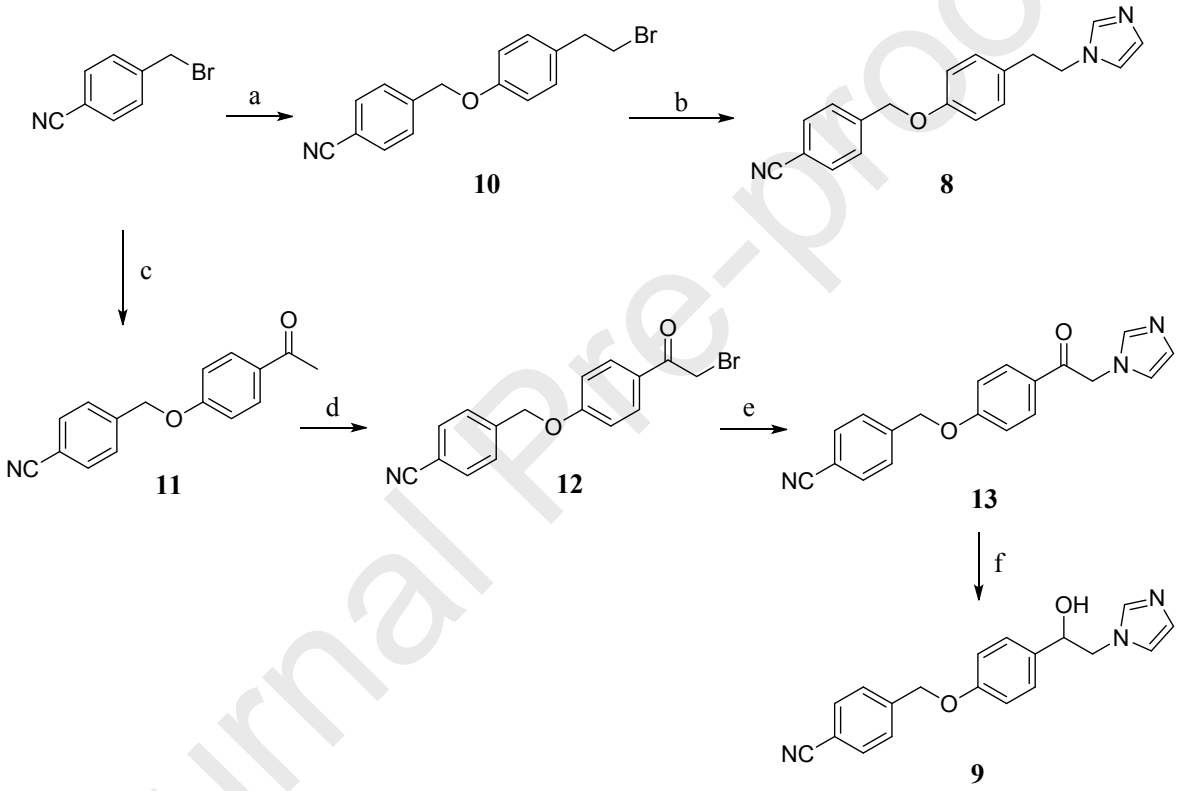

Scheme 1. Reagents and conditions: (a) 4-(2-bromoethyl)phenol, K_2CO_3, acetone, room temperature, 20 h; (b) imidazole, TEA, TBAB, CH_3CN dry, 90 °C, 45 min; (c) 1-(4-hydroxyphenyl)ethanone, K_2CO_3, acetone, room temperature, 20 h; (d) glacial acetic acid, HCl, Br_2, room temperature; (e) K_2CO_3, imidazole, DMF, room temperature, 2 h; (f) $NaBH_4$, CH_3OH, room temperature, reflux, 2 h.

2.3. HO inhibition and docking studies

The inhibitory activity of the newly synthesized compounds was measured using HO-1 and HO-2 isoforms extracted from rat spleen and rat brain microsomal fractions, respectively. The inhibitory

activity is reported as IC_{50} (μM), and obtained data are outlined in Table 1, employing azalanstat as the reference compound. All the compounds exhibited good inhibitory potency towards HO-1 and HO-2. Compound **9** showed remarkable HO-2 IC_{50} values <1 μM and interesting selectivity towards HO-1 (SI >15). Furthermore, a comparison between the HO-2 IC_{50} values of compound **9** and clemizole highlights that the former is about 5-fold more potent than clemizole (0.9 μM *vs* 3.4 μM, respectively), but less selective in terms of HO-1 inhibition.

Table 1
Chemical structures of rationally designed compounds **8** and **9** starting from known HO-1 inhibitors **5** and **7** and experimental IC_{50} values and selectivity index (SI) of compounds **8**, **9**, and **13** towards HO-1 and HO-2.

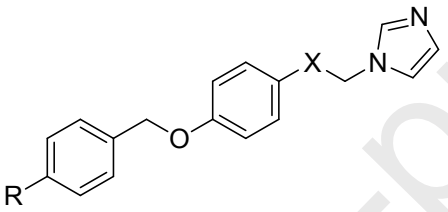

Compound	R	X	HO-1 IC_{50} (μM) [a]	HO-2 IC_{50} (μM) [a]	SI (HO-1/HO-2)	Volume
5	H	CHOH	0.50 ±0.01 [b]	11.7 ±0.9	0.04	316.81 A^3
7	H	CH_2	0.9 ±0.07 [c]	ND	ND	309.44 A^3
8	CN	CH_2	50.5 ±0.8	56.1 ±1.6	0.90	328.96 A^3
9	CN	CHOH	14.9 ±0.5	0.9 ±0.06	16.6	336.32 A^3
13	CN	C=O	75.4 ±1.2	72.8 ±2.0	1.04	ND
Azalanstat [c]			5.30 ±0.4	24.40 ±0.8	0.23	ND

[a] Data are reported as IC_{50} values in μM ±standard deviation (SD). Values are the mean of triplicate experiments. [b] Data from reference [37], [c] data from reference [34].

A docking study was performed to rationalize the obtained results. Docking was performed as described in the experimental section. The two binding pockets HO-1 and HO-2 were analyzed and aligned, resulted in a mean RMSD of 0.71 and a sequence identity of 77% (Table S1).

The results of the docking calculations are collected in Table 2, and the docking poses are shown in Figures 4 and S1–8. All of the studied compounds are located inside the binding pockets of both

proteins with the nitrogen atom of the imidazole rings in the proximity of the ferrous iron of heme, and the calculated binding energies are in the right relationship with the measured ones (Table 2). In this way, the iron is protected from oxidation, and the enzymes are not able to perform their activity. The three different molecules (**8**, **13**, and **9**) have similar interactions within the same binding pocket of HO-1 as well as HO-2. However, it is interesting to notice that the molecules interact differently in the two different binding pockets, as reported in Figure 4. All the molecules inside the HO-1 interact in a similar way of classical HO-1 inhibitors, where the aromatic groups are in the principal western binding pocket (Phe37, Met34, Val50, Leu147, Ala151, Phe166, Phe167, Phe214).

Interestingly, the molecules inside the HO-2 are differently positioned, although the first aromatic ring can occupy the same spot inside the pocket, the terminal aromatic ring of all compounds is not located inside the principal western region but is located in the secondary western region of the HO-2. Interesting to notice that the Phe167 controls the gate access to the western region in HO-1 that is substituted by Tyr187 in HO-2. The presence of the Tyr187 closes the access for the principal western region and drives the terminal ring in the secondary western region of HO-2. The presence of the consensus water molecule inside the binding pockets was also studied. In fact, a similarly located consensus water molecule (that mediates the interaction with Thr135 in HO-1) is present in HO-2 interacting with Thr155. We already reported this consensus water molecule as a key factor in the enantiomer recognition for HO-1 [43]. For molecule **9**, in both the studied proteins, the consensus water can mediate an interaction between Thr135/155 and the hydroxyl group of **9**. In particular, the stronger interaction is the one with the *R*-enantiomer. Analyzing the binding pose of the most potent compound inside the HO-2 (Figure 5), it is possible to see that the compound is optimally placed inside the binding pocket interacting with Thr155 (thought the consensus water) and with the Tyr 187, in this way **9** has optimum contact with the binding pocket residues of HO-2 and reach the highest binding energy value. The binding pose of this compound could be exploited for future designed HO-2 selective molecules based on a similar structure and targeting the consensus water and Tyr187 while occupying the secondary western region.

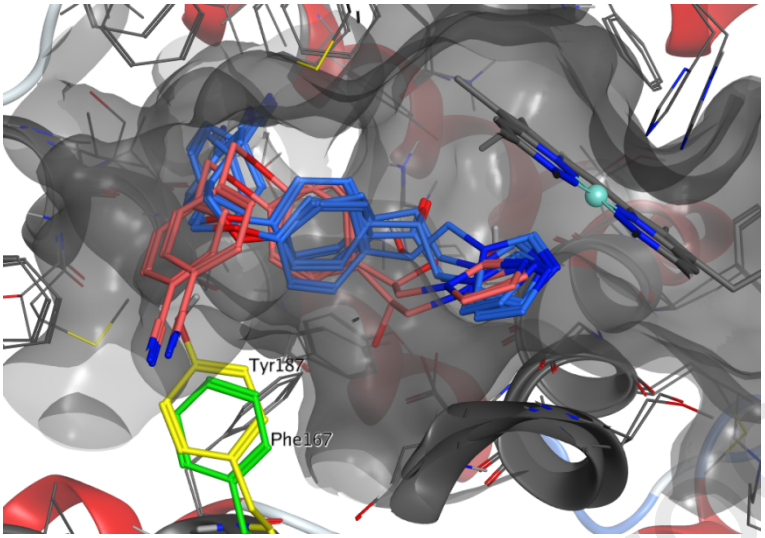

Figure 4. Binding poses of **8**, **13**, and **9** (*R* and *S*) in the aligned HO-1 and HO-2 binding pockets. In light red, the molecules inside HO-1, and in light blue the molecules inside HO-2. In yellow, the HO-2 Tyr187 and green the HO-1 Phe167.

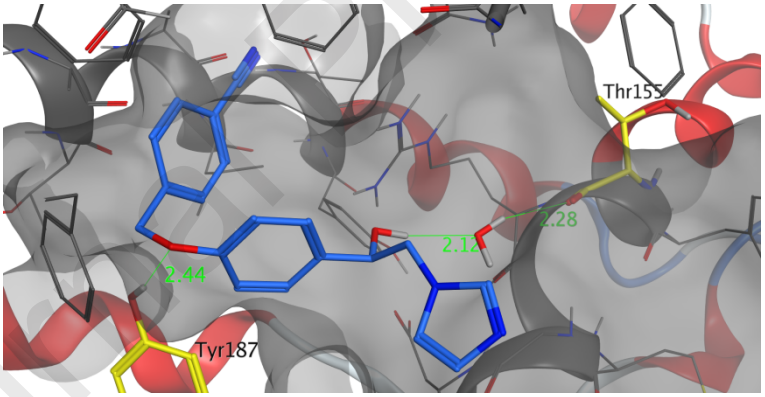

Figure 5. Binding poses of (*R*)-**9** in HO-2 binding pockets. Heme is removed for clarity, and Tyr187 and Thr155 are highlighted in yellow. The consensus water molecule is mediating an interaction between Thr155 and the -OH group of **9**.

Table 2
Docking results for the studied molecules **8**, **13**, and **9** (*R* and *S*).

Compound	HO-1 ΔG_B calcd. kcal/mol (K_i calcd. μM)	HO-2 ΔG_B calcd. kcal/mol (K_i calcd. μM)
8	−5.82 (54.83)	−5.77 (58.67)
13	−5.40 (109.59)	−5.48 (95.74)

(*R*)-9	−6.60 (14.44)	−8.16 (1.03)
(*S*)-9	−6.23 (26.98)	−7.81 (1.87)

2.4. ADMET assessment

To help us for a future selection of lead compounds and to further corroborate the molecular modeling and the in vitro evaluation, we also performed an in-silico absorption, distribution, metabolism, and excretion-toxicity (ADMET) pharmacokinetics evaluation. The *in-silico* assessment has been generated through the evaluation of pharmacokinetic profiles and possible adverse side effects for the molecules **8**, **9** and **13**. ADMET molecular studies were conducted using SwissADME (http://swissadme.ch) [44] and pkCSM (http://biosig.unimelb.edu.au/pkcsm/) [45], results are reported in the supporting information (Figures S9-S14).

All the three compounds resulted as orally available, with high gastrointestinal absorption and highly soluble in water. None of the compounds resulted as P-glycoprotein substrates; differently, most of the compounds are inhibitors of the CYP family proteins. Interestingly all of the compounds have no violation of the Lipinski rule of 5; they also have no violation of other drug-likeness rules (Ghose, Egan, Veber, and Muegee) [46-49]. The absorption and distribution calculated parameters have been depicted by the Edan–Egg model in Figure 6 (Brain or IntestinaL EstimateD, BOILED-Egg). The Edan-Egg model highlights that all compounds were predicted to passively permeate the blood-brain barrier and are not predicted to be effluated from the CNS by the P-glycoprotein. pkCSM calculated absorption properties showed a higher than 94% intestinal absorption due to the optimal (> 0.90) Caco-2 cell permeability. Moreover, most of the compounds can be absorbed by the skin (exploitable for transdermal drug delivery), as showed by the Log K_p < −2.5.

The calculated values of the total clearance indicate that most of the compounds have a good renal elimination (1.07–1.11 mL/min kg) and all of them are substrates of the renal organic cation transporter 2. pkCSM calculated toxicity properties did not point out concerns about the AMES test. However, compounds **9** and **13** were predicted as hepatotoxic, and all compounds are predicted as

inhibitors of the hERG II. On the other hand, the compounds have not skin sensitisation properties and are not inhibitors of the hERG I.

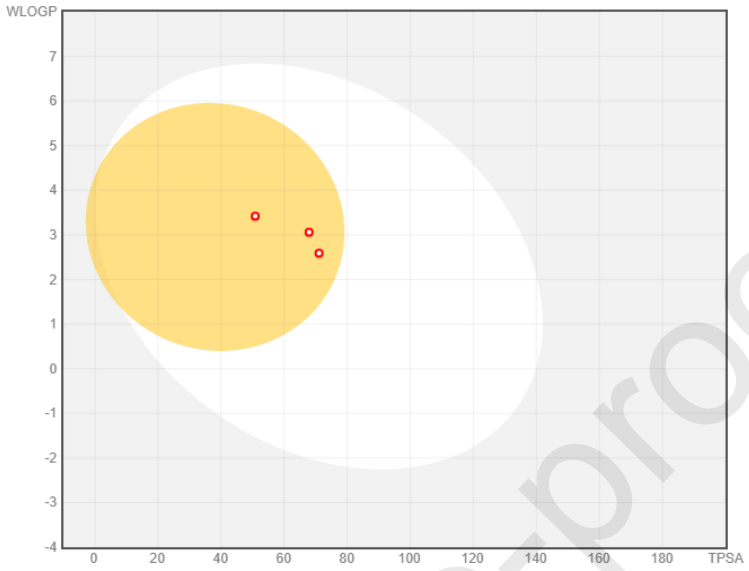

Figure 6. BOILED-Egg plot. Points located in the BOILED-Egg's yellow are the compounds predicted to permeate the BBB passively; differently, the ones in the white are the molecules predicted to be only passively absorbed by the gastrointestinal tract. Blue dots indicate molecules expected to be refluxed from the central nervous system (CNS) by the P-glycoprotein, whereas the red ones are not transported by the P-glycoprotein.

3. Conclusions

The present study was aimed at unraveling the chemical requirements to obtain new selective HO-2 inhibitors. To this extent, we rationally designed a small, focused series of derivatives by playing with the volume of the molecules. Starting from HO-1 inhibitors previously reported in the literature and by merely increasing the volume of the western region, we switched the inhibition preference from HO-1 to HO-2. Molecular modeling studies helped in understanding the binding mode of these compounds, highlighting that the molecules correctly interact with the HO-1 and HO-2 binding site. The molecular modeling showed that the molecules differently interact with the two binding sites and

that the presence of the HO-2 Tyr187 should represent the main reason for such a differentiation. Moreover, the consensus water molecule present in both binding sites can mediate an interaction with a Thr155 for the *R* enantiomer mainly. This set of described interactions can be useful for the design of new selective HO-2 compounds.

4. Experimental section

4.1. Chemistry

Reactions were followed by TLC carried out on Sigma Aldrich silica plates (60 F254), using UV light (254 nm and 366 nm) for visualization and developed using I_2 chamber. Flash chromatographic purification on glasses columns was achieved employing Merck silica gel 60, 0.040–0.063 mm (230–400 mesh). Chemical syntheses requiring microwave irradiation were performed with a CEM Discover instrument using closed Pyrex glass tubes (ca. 10 mL) with Teflon-coated septa. Melting points were assigned by using an IA9200 Electrothermal apparatus furnished with a digital thermometer in capillary glass tubes and are uncorrected. Infrared spectra were recorded on a spectrometer in KBr disks or NaCl crystal windows. ^{1}H NMR spectra were recorded on a 200 or 500 MHz spectrometer in DMSO-d_6 solution. Chemical shifts are given in δ values (ppm), using tetramethylsilane (TMS) as the internal standard; coupling constants (*J*) are given in Hz. Signal multiplicities are characterized as s (singlet), d (doublet), t (triplet), q (quartet), m (multiplet), br (broad). Elemental analyses for C, H, N, and O were within ±0.4% of theoretical values and were accomplished through a Carlo Erba Elemental Analyzer Mod. 1108 apparatus. Reagents, solvents, and starting materials were acquired from commercial suppliers.

*4.1.1. 4-[[4-(2-Bromoethyl)phenoxy]methyl]benzonitrile (**10**)*

A mixture of 4-(bromomethyl)benzonitrile (3.5 mmol), 4-(2-bromoethyl)phenol (6.9 mmol), and K_2CO_3 (6.9 mmol) in acetone (20 mL) was left stirring for 20 h, at room temperature. Then it was evaporated to dryness, added with deionized water (40 mL). The obtained suspension was left stirring for 15 min, filtered under vacuum, and washed twice with cold water. The white solid was left in the

stove at 50 °C and crystallized using C_2H_5OH as solvent. The title compound was obtained as a pure white solid (59%): mp 90–92 °C; ^{1}H NMR (200 MHz, DMSO-d_6): δ 7.87 (d, J = 8.2 Hz, 2H aromatic), 7.63 (d, J = 8 Hz, 2H aromatic), 7.20 (d, J = 8.2 Hz, 2H, aromatic), 6.95 (d, J = 8.4 Hz, 2H, aromatic), 5.20 (s, 2H, CH_2O), 3.67 (t, J = 7.2 Hz, 2H, CH_2CH_2), 3.05 (t, J = 7.2 Hz, 2H, CH_2CH_2). Anal. Calcd. for ($C_{16}H_{14}BrNO$): C, 60.78; H, 4.46; N, 4.43. Found: C, 60.69; H, 4.48; N, 4.19.

*4.1.2. 4-[[4-[2-(1H-Imidazol-1yl)ethyl]phenoxy]methyl]benzonitrile (**8**)*

Compound **10** (0.95 mmol) was dissolved in anhydrous CH_3CN (5 mL). Then, imidazole (1.4 mmol), TEA (0.95 mmol) and TBAB (0.95 mmol) were added and the reaction mixture was left refluxing for 45 min in microwave (90 °C, 200 W, 150 Psi). The mixture was concentrated and the residue was dissolved in EtOAc (100 mL), washed with NaOH 0.1 N (3×50 mL) and brine (1×50 mL). The organic layer was dried over anhydrous Na_2SO_4, filtered and concentrated under vacuum. The obtained yellow oil was purified by flash chromatography (9.5 EtOAc/0.5 CH_3OH) affording a pure white solid (32%): mp 110–112 °C; ^{1}H NMR (500 MHz, DMSO-d_6): δ 7.86 (d, J = 8.4 Hz, 1H + 1H, aromatic + imidazole), 7.63 (d, J = 8.4 Hz, 2H, aromatic), 7.47 (s, 1H, imidazole), 7.12 (s, 1H, imidazole), 7.09 (d, J = 8.6 Hz, 2H, aromatic), 6.92 (d, J = 8.6 Hz, 2H), 6.84 (s, 2H, imidazole), 5.18 (s, 2H, CH_2O), 4.15 (t, J = 7.3 Hz, 2H, CH_2CH_2), 2.95 (t, J = 7.3 Hz, 2H, CH_2CH_2). ^{13}C NMR (125 MHz, DMSO-d_6) 156.52, 142.98, 132.33, 130.63, 129.67, 128.16, 127.98, 119.09, 118.69, 114.64, 110.36, 68.14, 47.29, 35.82. Anal. Calcd. for ($C_{19}H_{17}N_3O$): C, 75.23; H, 5.65; N, 13.85. Found: C, 74.92; H, 5.66; N, 13.91.

*4.1.3. 4-[(4-Acetylphenoxy)methyl]benzonitrile (**11**)*

A mixture of the appropriate commercially available 1-(4-hydroxyphenyl)ethanone (10 mmol) and 4-(bromomethyl)benzonitrile (10 mmol), in acetone (40 mL) and in the presence of K_2CO_3 (20 mmol) and a catalytic amount of KI was refluxed for 3 h. The reaction was checked for completion by TLC (7 Cy/3 EtOAc), and then, the solvent was evaporated. Distilled water was added, and the suspension was left stirring for 15 min, filtered and washed with water to obtain an off-white solid that was

recrystallized from C_2H_5OH. Analytical characterization is in agreement with previously reported data [50].

*4.1.4. 4-[[4-(Bromoacetyl)phenoxy]methyl]benzonitrile (**12**)*

4-[(4-Acetylphenoxy)methyl]benzonitrile **11** (5 mmol) was dissolved in glacial acetic acid (20 mL) and 0.5 mL of conc. HCl, then bromine (5 mmol) was added dropwise. The mixture was left stirring at room temperature until colorless. The obtained solution was dropped in saturated $NaHCO_3$, and the pH was adjusted to 9. The suspension obtained was filtered in vacuum to obtain a white solid. The residue was dissolved in DCM and washed with brine. The organic layer was dried over Na_2SO_4, filtered, and concentrated. The obtained crude **12** was used as such in the following step.

*4.1.5. 4-[[4-(1H-Imidazol-1-ylacetyl)phenoxy]methyl]benzonitrile (**13**)*

4-[[4-(Bromoacetyl)phenoxy]methyl]benzonitrile **12** (5 mmol), was dissolved in anhydrous DMF (15 mL) and added dropwise to a previously prepared suspension of imidazole (15 mmol) and K_2CO_3 (15 mmol) in anhydrous DMF (20 mL). The obtained reaction mixture was left stirring for 2 h; then, water was added and the resulting suspension was filtered in vacuum. The obtained crude material was purified by column chromatography using 9.5 EtOAc/0.5 CH_3OH as eluent. The residue was recrystallized from EtOAc to obtain a pure yellow solid (74%): mp 178–180 °C; ^{1}H NMR (500 MHz, DMSO-d_6): δ 8.01 (d, J = 8.9 Hz, 2H, aromatic), 7.87 (d, J = 8.3 Hz, 2H, aromatic), 7.66 (d, J = 8.3 Hz, 2H, aromatic), 7.57 (s, 1H, imidazole), 7.19 (d, J = 8.9 Hz, 2H, aromatic), 7.09 (s, 1H, imidazole), 6.91 (s, 1H, imidazole), 5.66 (s, 2H, CH_2N), 5.35 (s, 2H, CH_2O). ^{13}C NMR (125 MHz, DMSO-d_6) 191.95, 162.33, 142.25, 138.40, 132.54, 130.44, 128.23, 127.82, 127.80, 121.01, 118.77, 115.05, 110.73, 68.63, 52.28. Anal. Calcd. for ($C_{19}H_{15}N_3O_2$): C, 71.91; H, 4.76; N, 13.24. Found: C, 72.21; H, 4.79; N, 13.19.

*4.1.6. 4-[[4-[1-hydroxy-2-(1H-imidazol-1-yl)ethyl]phenoxy]methyl]benzonitrile (**9**)*

A mixture of the imidazole-ketone **13** (0.63 mmol) and $NaBH_4$ (1.26 mmol) in anhydrous CH_3OH (10 mL) was refluxed for 2 h; then it was evaporated to dryness, added with deionized water (40 mL), acidified with HCl 1 N and heated to 110 °C for 0.5 h. After cooling to room temperature, the reaction

mixture was treated with a 1 N NaOH solution up to a pH of 8.5 and the obtained suspension was filtered, washed repeatedly with water to neutrality, dried and crystallized from C_2H_5OH. The title compound was obtained as pure off-white solid (89%): mp 165-166 °C. ^{1}H NMR (500 MHz, DMSO-d_6): δ 7.86 (d, J = 8.2 Hz, 2H, aromatic), 7.62 (d, J = 8.2 Hz, 2H, aromatic), 7.48 (s, 1H, imidazole), 7.25 (d, J = 8.6 Hz, 2H, aromatic), 7.09 (s, 1H, imidazole), 6.96 (d, J = 8.6 Hz, 2H, aromatic) , 6.81 (s, 1H, imidazole), 5.63 (d, J = 3.9 Hz, 1H, OH), 5.20 (s, 2H, CH_2O), 4.78 – 4.71 (m, 1H, CHOH), 4.08 (dd, J = 13.9, J = 4 Hz, 1H, CH_ACH_B), 4.00 (dd, J = 13.9, J = 8 Hz, 1H, CH_ACH_B). ^{13}C NMR (125 MHz, DMSO-d_6) 157.23, 143.05, 135.25, 132.46, 129.37, 128.07, 127.69, 127.33, 120.08, 118.83, 114.43, 110.44, 71.65, 68.20, 53.59. Anal. Calcd. for ($C_{19}H_{17}N_3O_2$): C, 71.46; H, 5.37; N, 13.16. Found: C, 71.13; H, 5.33; N, 13.26

4.2. Biology

4.2.1. Preparation of spleen and brain microsomal fractions

Rat spleen and brain microsomal fractions were prepared by differential centrifugation to obtain HO-1 and HO-2, respectively; the dominance of HO-1 protein in the rat spleen and of HO-2 in the rat brain has been widely documented [51]. Rat spleen and brain microsomal fractions were selected in order to use the most native (*i.e.*, closest to *in vivo*) forms of HO-1 and HO-2. Spleen and brain (Sprague-Dawley rats) microsomal fractions were prepared according to the procedure outlined by Ryter et al. [52]. The experiments reported in the present paper complied with current Italian law and met the guidelines of the Institutional Animal Care and Use Committee of MINISTRY OF HEALTH (Directorate General for Animal Health and Veterinary Medicines) (Italy). The experiments were performed in male Sprague-Dawley albino rats (150 g body weight and age 45 d). Animals had free access to water and were maintained in a temperature- and light-controlled facility. Each rat was sacrificed and their spleen and brain were excised, weighed and pooled to obtain homogenates. Spleen and brain homogenates (15%, w/v) pooled from four rats was prepared in ice-cold HO-homogenizing buffer (50 mM Tris buffer, pH 7.4, containing 0.25 M sucrose) using a Potter-Elvehjem homogenizing system with a Teflon pestle. Centrifugation at 10,000g for 20 min at 4 °C, followed by

centrifugation of the supernatant at 100,000g for 60 min at 4 °C was used to obtain microsomal fraction of rat spleen and brain homogenates. The 100,000g pellet (microsomes) was resuspended in 100 mM potassium phosphate buffer, pH 7.8, containing 2 mM $MgCl_2$ with a Potter-Elvehjem homogenizing system. Equal aliquots of the rat spleen and brain microsomal fractions were and stored at −80 °C for up to 2 months. Protein concentration was measured using TAKE 3 nanodrop.

4.2.2. Preparation of biliverdin reductase

Biliverdin reductase (BVR) was obtained from the liver cytosol. Rat liver was perfused through the hepatic portal vein with cold 0.9% NaCl; then, it was cut and perfused with 2×20 mL of ice-cold PBS to remove all of the blood. Liver homogenates were obtained with 3 volumes of a solution containing 1.15% KCl w/v and Tris buffer 20 mM, pH 7.8 on ice. Homogenates were centrifuged at 10,000g for 20 minutes at 4 °C and then the supernatant was centrifuged at 100,000g for 1 h at 4 °C to sediment the microsomes. Small amounts of the 100,000g supernatant were stored at −80 °C after its protein concentration was measured.

4.2.3. Measurement of HO-1 and HO-2 enzymatic activities in the microsomal fraction of rat spleen and brain

The HO-1 and HO-2 activities were measured following the bilirubin formation, as described by Ryter et al. [52]. Reaction mixtures (500 μL) contained: 20 mM Tris-HCl, pH 7.4, (1 mg/mL) microsomal extract, 0.5–2.0 mg/mL biliverdin reductase, 1 mM NADPH, 2 mM glucose 6-phosphate (G6P), 1 U G6P dehydrogenase, 25 μM hemin, 10 μL of DMSO (or the same volume of DMSO solution of test compounds to a final concentration of 100, 10, and 1 μM). 60 min incubations at 37 °C were carried out in a circulating water bath in the dark. 1 volume of chloroform was added to stop reactions. After recovering the chloroform phase, the amount of bilirubin formed was measured with a double-beam spectrophotometer as OD464-530 nm (extinction coefficient, 40 mM/cm^{-1} for bilirubin). One unit of the enzyme was defined as the amount of enzyme catalyzing the formation of 1 nmol of bilirubin/mg protein/h.

4.3. Computational methods

The three-dimensional structures of all the studied molecules were generated using Marvin Sketch (18.24, ChemAxon Ltd., Budapest, Hungary) [53]. The input 2D structures were minimized using the Merck molecular force field (MMFF94) present in Marvin Sketch at neutral pH. Then, the obtained geometries were further optimized using the PM3 Hamiltonian in MOPAC (MOPAC2016 v. 18.151, Stewart Computational Chemistry, Colorado Springs, CO, USA) [54]. The docking model was validated as we already published in a different paper using the classical inhibitors of HO-1 (Azalanstat, QC-15, QC-80, QC-82, QC-86, and QC-308) [37]. The protein and the ligands were prepared using YASARA (v. 19.5.5, YASARA Biosciences GmbH, Vienna, Austria). The protein structures were downloaded from the protein data bank (https://www.rcsb.org/, ID: 2DY5 for HO-1 and 2QPP for HO-2). Chain A and the heme group were maintained for HO-1, while chain B was used for HO-2. All the water molecules were removed apart from the described consensus water [43]. In the docking experiments, the amino acid residues of the proteins were kept rigid; differently, the single bonds of the ligands were kept free to rotate. Docking was performed by applying the Lamarckian genetic algorithm (LGA) implemented in AutoDock using YASARA GUI. The ligand-centered maps were generated by the AutoGrid with a spacing of 0.375Å and dimensions that surround all atoms extending 5Å from the surface of the ligand in a cuboid box. All of the parameters were at their default settings.

Supplementary data

Supplementary data related to this article can be found at

Acknowledgements

This work was supported by 1) Research Funding for University (Piano per la Ricerca 2016–2018, project code 57722172107 and Programma Ricerca di Ateneo UNICT 2020--22 linea 2); 2) Project authorized by the Ministry of Health (Directorate General for Animal Health and Veterinary

Medicines) “Dosing of enzymatic activities in rat microsomes” (2018–2022) (project code 02769.N.VLY); 3) PON R&I funds 2014-2020 (CUP: E66C18001320007, AIM1872330, activity 1).

References

1. Abraham, N. G.; Kappas, A., Pharmacological and clinical aspects of heme oxygenase. *Pharmacol Rev.* **2008**, 60, (1), 79-127.
2. Ewing, J. F.; Maines, M. D., Histochemical localization of heme oxygenase-2 protein and mRNA expression in rat brain. *Brain Res Brain Res Protoc.* **1997**, 1, (2), 165-74.
3. Battino, M.; Giampieri, F.; Pistollato, F.; Sureda, A.; de Oliveira, M. R.; Pittala, V.; Fallarino, F.; Nabavi, S. F.; Atanasov, A. G.; Nabavi, S. M., Nrf2 as regulator of innate immunity: A molecular Swiss army knife! *Biotechnol Adv.* **2018**, 36, (2), 358-370.
4. Amata, E.; Pittala, V.; Marrazzo, A.; Parenti, C.; Prezzavento, O.; Arena, E.; Nabavi, S. M.; Salerno, L., Role of the Nrf2/HO-1 axis in bronchopulmonary dysplasia and hyperoxic lung injuries. *Clin Sci (Lond).* **2017**, 131, (14), 1701-1712.
5. Bauer, M.; Bauer, I., Heme oxygenase-1: redox regulation and role in the hepatic response to oxidative stress. *Antioxid. Redox Signal.* **2002**, 4, (5), 749-58.
6. Carota, G.; Raffaele, M.; Sorrenti, V.; Salerno, L.; Pittala, V.; Intagliata, S., Ginseng and heme oxygenase-1: The link between an old herb and a new protective system. *Fitoterapia* **2019**, 139, 104370.
7. Pittala, V.; Salerno, L.; Romeo, G.; Acquaviva, R.; Di Giacomo, C.; Sorrenti, V., Therapeutic Potential of Caffeic Acid Phenethyl Ester (CAPE) in Diabetes. *Curr. Med. Chem.* **2018**, 25, (37), 4827-4836.
8. Pittala, V.; Salerno, L.; Romeo, G.; Siracusa, M. A.; Modica, M. N.; Romano, G. L.; Salomone, S.; Drago, F.; Bucolo, C., Effects of novel hybrids of caffeic acid phenethyl ester and NSAIDs on experimental ocular inflammation. *Eur. J. Pharmacol.* **2015**, 752, 78-83.
9. Pittala, V.; Vanella, L.; Salerno, L.; Di Giacomo, C.; Acquaviva, R.; Raffaele, M.; Romeo, G.; Modica, M. N.; Prezzavento, O.; Sorrenti, V., Novel Caffeic Acid Phenethyl Ester (Cape) Analogues as Inducers of Heme Oxygenase-1. *Curr. Pharm. Des.* **2017**, 23, (18), 2657-2664.
10. Pittala, V.; Vanella, L.; Salerno, L.; Romeo, G.; Marrazzo, A.; Di Giacomo, C.; Sorrenti, V., Effects of Polyphenolic Derivatives on Heme Oxygenase-System in Metabolic Dysfunctions. *Curr. Med. Chem.* **2018**, 25, (13), 1577-1595.
11. Pittala, V.; Vanella, L.; Maria Platania, C. B.; Salerno, L.; Raffaele, M.; Amata, E.; Marrazzo, A.; Floresta, G.; Romeo, G.; Greish, K.; Intagliata, S.; Bucolo, C.; Sorrenti, V., Synthesis, in vitro and in silico studies of HO-1 inducers and lung antifibrotic agents. *Future Med. Chem.* **2019**, 11, (13), 1523-1536.
12. Ferrandiz, M. L.; Devesa, I., Inducers of heme oxygenase-1. *Curr. Pharm. Des.* **2008**, 14, (5), 473-86.
13. Chau, L. Y., Heme oxygenase-1: emerging target of cancer therapy. *J. Biomed. Sci.* **2015**, 22, 22.
14. Podkalicka, P.; Mucha, O.; Jozkowicz, A.; Dulak, J.; Loboda, A., Heme oxygenase inhibition in cancers: possible tools and targets. *Contemp Oncol (Pozn).* **2018**, 22, (1A), 23-32.
15. Dichiara, M.; Prezzavento, O.; Marrazzo, A.; Pittala, V.; Salerno, L.; Rescifina, A.; Amata, E., Recent advances in drug discovery of phototherapeutic non-porphyrinic anticancer agents. *Eur. J. Med. Chem.* **2017**, 142, 459-485.
16. Salerno, L.; Pittala, V.; Romeo, G.; Modica, M. N.; Siracusa, M. A.; Di Giacomo, C.; Acquaviva, R.; Barbagallo, I.; Tibullo, D.; Sorrenti, V., Evaluation of novel aryloxyalkyl

derivatives of imidazole and 1,2,4-triazole as heme oxygenase-1 (HO-1) inhibitors and their antitumor properties. *Bioorg. Med. Chem.* **2013**, 21, (17), 5145-53.
17. Salerno, L.; Romeo, G.; Modica, M. N.; Amata, E.; Sorrenti, V.; Barbagallo, I.; Pittala, V., Heme oxygenase-1: A new druggable target in the management of chronic and acute myeloid leukemia. *Eur. J. Med. Chem.* **2017**, 142, 163-178.
18. Berberat, P. O.; Dambrauskas, Z.; Gulbinas, A.; Giese, T.; Giese, N.; Kunzli, B.; Autschbach, F.; Meuer, S.; Buchler, M. W.; Friess, H., Inhibition of heme oxygenase-1 increases responsiveness of pancreatic cancer cells to anticancer treatment. *Clin. Cancer Res.* **2005**, 11, (10), 3790-8.
19. Salerno, L.; Pittala, V.; Romeo, G.; Modica, M. N.; Marrazzo, A.; Siracusa, M. A.; Sorrenti, V.; Di Giacomo, C.; Vanella, L.; Parayath, N. N.; Greish, K., Novel imidazole derivatives as heme oxygenase-1 (HO-1) and heme oxygenase-2 (HO-2) inhibitors and their cytotoxic activity in human-derived cancer cell lines. *Eur. J. Med. Chem.* **2015**, 96, 162-72.
20. Barbagallo, I.; Giallongo, C.; Li Volti, G.; Distefano, A.; Camiolo, G.; Raffaele, M.; Salerno, L.; Pittala, V.; Sorrenti, V.; Avola, R.; Di Rosa, M.; Vanella, L.; Di Raimondo, F.; Tibullo, D., Heme Oxygenase Inhibition Sensitizes Neuroblastoma Cells to Carfilzomib. *Mol. Neurobiol.* **2019**, 56, (2), 1451-1460.
21. Castruccio Castracani, C.; Longhitano, L.; Distefano, A.; Di Rosa, M.; Pittala, V.; Lupo, G.; Caruso, M.; Corona, D.; Tibullo, D.; Li Volti, G., Heme Oxygenase-1 and Carbon Monoxide Regulate Growth and Progression in Glioblastoma Cells. *Mol. Neurobiol.* **2020**, 57, (5), 2436-2446.
22. Ciaffaglione, V.; Intagliata, S.; Pittala, V.; Marrazzo, A.; Sorrenti, V.; Vanella, L.; Rescifina, A.; Floresta, G.; Sultan, A.; Greish, K.; Salerno, L., New Arylethanolimidazole Derivatives as HO-1 Inhibitors with Cytotoxicity against MCF-7 Breast Cancer Cells. *Int. J. Mol. Sci.* **2020**, 21, (6), 1923.
23. Greish, K. F.; Salerno, L.; Al Zahrani, R.; Amata, E.; Modica, M. N.; Romeo, G.; Marrazzo, A.; Prezzavento, O.; Sorrenti, V.; Rescifina, A.; Floresta, G.; Intagliata, S.; Pittala, V., Novel Structural Insight into Inhibitors of Heme Oxygenase-1 (HO-1) by New Imidazole-Based Compounds: Biochemical and In Vitro Anticancer Activity Evaluation. *Molecules* **2018**, 23, (5), 1209.
24. Raffaele, M.; Pittala, V.; Zingales, V.; Barbagallo, I.; Salerno, L.; Li Volti, G.; Romeo, G.; Carota, G.; Sorrenti, V.; Vanella, L., Heme Oxygenase-1 Inhibition Sensitizes Human Prostate Cancer Cells towards Glucose Deprivation and Metformin-Mediated Cell Death. *Int. J. Mol. Sci.* **2019**, 20, (10), 2593.
25. Sorrenti, V.; Pittala, V.; Romeo, G.; Amata, E.; Dichiara, M.; Marrazzo, A.; Turnaturi, R.; Prezzavento, O.; Barbagallo, I.; Vanella, L.; Rescifina, A.; Floresta, G.; Tibullo, D.; Di Raimondo, F.; Intagliata, S.; Salerno, L., Targeting heme Oxygenase-1 with hybrid compounds to overcome Imatinib resistance in chronic myeloid leukemia cell lines. *Eur. J. Med. Chem.* **2018**, 158, 937-950.
26. Spampinato, M.; Sferrazzo, G.; Pittala, V.; Di Rosa, M.; Vanella, L.; Salerno, L.; Sorrenti, V.; Carota, G.; Parrinello, N.; Raffaele, M.; Tibullo, D.; Li Volti, G.; Barbagallo, I., Non-competitive heme oxygenase-1 activity inhibitor reduces non-small cell lung cancer glutathione content and regulates cell proliferation. *Mol. Biol. Rep.* **2020**, 47, (3), 1949-1964.
27. Intagliata, S.; Salerno, L.; Ciaffaglione, V.; Leonardi, C.; Fallica, A. N.; Carota, G.; Amata, E.; Marrazzo, A.; Pittala, V.; Romeo, G., Heme Oxygenase-2 (HO-2) as a therapeutic target: Activators and inhibitors. *Eur. J. Med. Chem.* **2019**, 183, 111703.
28. Trakshel, G. M.; Kutty, R. K.; Maines, M. D., Purification and characterization of the major constitutive form of testicular heme oxygenase. The noninducible isoform. *J. Biol. Chem.* **1986**, 261, (24), 11131-7.

29. Salerno, L.; Floresta, G.; Ciaffaglione, V.; Gentile, D.; Margani, F.; Turnaturi, R.; Rescifina, A.; Pittala, V., Progress in the development of selective heme oxygenase-1 inhibitors and their potential therapeutic application. *Eur. J. Med. Chem.* **2019**, 167, 439-453.
30. Rahman, M. N.; Vukomanovic, D.; Vlahakis, J. Z.; Szarek, W. A.; Nakatsu, K.; Jia, Z. C., Structural insights into human heme oxygenase-1 inhibition by potent and selective azole-based compounds. *J. R. Soc. Interface* **2013**, 10, (78), 20120697.
31. Pittala, V.; Salerno, L.; Romeo, G.; Modica, M. N.; Siracusa, M. A., A focus on heme oxygenase-1 (HO-1) inhibitors. *Curr. Med. Chem.* **2013**, 20, (30), 3711-32.
32. Rahman, M. N.; Vlahakis, J. Z.; Vukomanovic, D.; Lee, W.; Szarek, W. A.; Nakatsu, K.; Jia, Z. C., A Novel, "Double-Clamp" Binding Mode for Human Heme Oxygenase-1 Inhibition. *Plos One* **2012**, 7, (1): e29514.
33. Rahman, M. N.; Vlahakis, J. Z.; Vukomanovic, D.; Szarek, W. A.; Nakatsu, K.; Jia, Z. C., X-ray Crystal Structure of Human Heme Oxygenase-1 with (2R,4S)-2-[2-(4-Chlorophenyl)ethyl]-2-[(1H-imidazol-1-yl)methyl]-4[((5-trifluoromethylpyridin-2-yl)thio)methyl]-1,3-dioxolane: A Novel, Inducible Binding Mode. *J. Med. Chem.* **2009**, 52, (15), 4946-4950.
34. Floresta, G.; Pittala, V.; Sorrenti, V.; Romeo, G.; Salerno, L.; Rescifina, A., Development of new HO-1 inhibitors by a thorough scaffold-hopping analysis. *Bioorg Chem.* **2018**, 81, 334-339.
35. Floresta, G.; Amata, E.; Gentile, D.; Romeo, G.; Marrazzo, A.; Pittala, V.; Salerno, L.; Rescifina, A., Fourfold Filtered Statistical/Computational Approach for the Identification of Imidazole Compounds as HO-1 Inhibitors from Natural Products. *Mar. Drugs* **2019**, 17, (2), 113.
36. Floresta, G.; Amata, E.; Dichiara, M.; Marrazzo, A.; Salerno, L.; Romeo, G.; Prezzavento, O.; Pittala, V.; Rescifina, A., Identification of Potentially Potent Heme Oxygenase 1 Inhibitors through 3D-QSAR Coupled to Scaffold-Hopping Analysis. *ChemMedChem* **2018**, 13, (13), 1336-1342.
37. Salerno, L.; Amata, E.; Romeo, G.; Marrazzo, A.; Prezzavento, O.; Floresta, G.; Sorrenti, V.; Barbagallo, I.; Rescifina, A.; Pittala, V., Potholing of the hydrophobic heme oxygenase-1 western region for the search of potent and selective imidazole-based inhibitors. *Eur. J. Med. Chem.* **2018**, 148, 54-62.
38. Amata, E.; Marrazzo, A.; Dichiara, M.; Modica, M. N.; Salerno, L.; Prezzavento, O.; Nastasi, G.; Rescifina, A.; Romeo, G.; Pittala, V., Comprehensive data on a 2D-QSAR model for Heme Oxygenase isoform 1 inhibitors. *Data Brief.* **2017**, 15, 281-299.
39. Amata, E.; Marrazzo, A.; Dichiara, M.; Modica, M. N.; Salerno, L.; Prezzavento, O.; Nastasi, G.; Rescifina, A.; Romeo, G.; Pittala, V., Heme Oxygenase Database (HemeOxDB) and QSAR Analysis of Isoform 1 Inhibitors. *ChemMedChem* **2017**, 12, (22), 1873-1881.
40. Mucha, O.; Podkalicka, P.; Mikulski, M.; Barwacz, S.; Andrysiak, K.; Biela, A.; Mieczkowski, M.; Kachamakova-Trojanowska, N.; Ryszawy, D.; Bialas, A.; Szelazek, B.; Grudnik, P.; Majewska, E.; Michalik, K.; Jakubiec, K.; Bien, M.; Witkowska, N.; Gluza, K.; Ekonomiuk, D.; Sitarz, K.; Galezowski, M.; Brzozka, K.; Dubin, G.; Jozkowicz, A.; Dulak, J.; Loboda, A., Development and characterization of a new inhibitor of heme oxygenase activity for cancer treatment. *Arch Biochem Biophys* **2019**, 671, 130-142.
41. Podkalicka, P.; Mucha, O.; Kruczek, S.; Biela, A.; Andrysiak, K.; Stepniewski, J.; Mikulski, M.; Galezowski, M.; Sitarz, K.; Brzozka, K.; Jozkowicz, A.; Dulak, J.; Loboda, A., Synthetically Lethal Interactions of Heme Oxygenase-1 and Fumarate Hydratase Genes. *Biomolecules* **2020**, 10, (1), 143.
42. Vlahakis, J. Z.; Vukomanovic, D.; Nakatsu, K.; Szarek, W. A., Selective inhibition of heme oxygenase-2 activity by analogs of 1-(4-chlorobenzyl)-2-(pyrrolidin-1-ylmethyl)-1H-benzimidazole (clemizole): Exploration of the effects of substituents at the N-1 position. *Bioorg. Med. Chem.* **2013**, 21, (21), 6788-6795.

43. Floresta, G.; Carotti, A.; Ianni, F.; Sorrenti, V.; Intagliata, S.; Rescifina, A.; Salerno, L.; Di Michele, A.; Sardella, R.; Pittala, V., Chromatograpic resolution of phenylethanolic-azole racemic compounds highlighted stereoselective inhibition of heme oxygenase-1 by (R)-enantiomers. *Bioorg Chem.* **2020**, 99, 103777.
44. Daina, A.; Michielin, O.; Zoete, V., SwissADME: a free web tool to evaluate pharmacokinetics, drug-likeness and medicinal chemistry friendliness of small molecules. *Sci Rep* **2017**, 7, 42717.
45. Pires, D. E.; Blundell, T. L.; Ascher, D. B., pkCSM: Predicting Small-Molecule Pharmacokinetic and Toxicity Properties Using Graph-Based Signatures. *J. Med. Chem.* **2015**, 58, (9), 4066-72.
46. Lipinski, C. A.; Lombardo, F.; Dominy, B. W.; Feeney, P. J., Experimental and computational approaches to estimate solubility and permeability in drug discovery and development settings. *Adv Drug Deliv Rev* **2001**, 46, (1-3), 3-26.
47. Ghose, A. K.; Viswanadhan, V. N.; Wendoloski, J. J., A knowledge-based approach in designing combinatorial or medicinal chemistry libraries for drug discovery. 1. A qualitative and quantitative characterization of known drug databases. *J. Comb. Chem.* **1999**, 1, (1), 55-68.
48. Egan, W. J.; Merz, K. M., Jr.; Baldwin, J. J., Prediction of drug absorption using multivariate statistics. *J. Med. Chem.* **2000**, 43, (21), 3867-77.
49. Veber, D. F.; Johnson, S. R.; Cheng, H. Y.; Smith, B. R.; Ward, K. W.; Kopple, K. D., Molecular properties that influence the oral bioavailability of drug candidates. *J. Med. Chem.* **2002**, 45, (12), 2615-23.
50. Ma, Y. T.; Fan, H. F.; Gao, Y. Q.; Li, H.; Zhang, A. L.; Gao, J. M., Natural Products as Sources of New Fungicides (I): Synthesis and Antifungal Activity of Acetophenone Derivatives Against Phytopathogenic Fungi. *Chem. Biol. Drug Des.* **2013**, 81, (4), 545-552.
51. Maines, M. D., Heme Oxygenase - Function, Multiplicity, Regulatory Mechanisms, and Clinical-Applications. *Faseb J.* **1988**, 2, (10), 2557-2568.
52. Ryter, S. W.; Alam, J.; Choi, A. M. K., Heme oxygenase-1/carbon monoxide: From basic science to therapeutic applications. *Physiol. Rev.* **2006**, 86, (2), 583-650.
53. Csizmadia, F., JChem: Java applets and modules supporting chemical database handling from web browsers. *J. Chem. Inf. Comput. Sci.* **2000**, 40, (2), 323-4.
54. Stewart, J. J., MOPAC: a semiempirical molecular orbital program. *J. Comput.-Aided Mol. Des.* **1990**, 4, (1), 1-105.

Declaration of interests

☒ The authors declare that they have no known competing financial interests or personal relationships that could have appeared to influence the work reported in this paper.

Graphical abstract

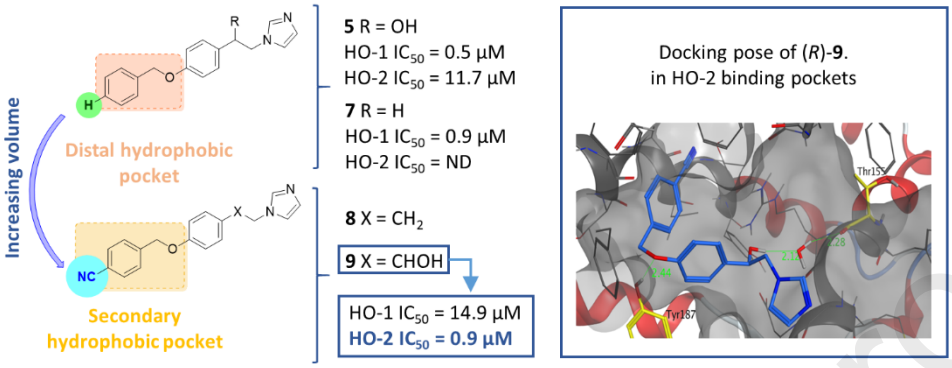

Identification of a potent heme oxygenase-2 (HO-2) inhibitor by targeting the secondary hydrophobic pocket of the HO-2 western region

Giuseppe Floresta [a, b], Antonino N. Fallica [a], Giuseppe Romeo [a], Valeria Sorrenti [a], Loredana Salerno [a], Antonio Rescifina [a], Valeria Pittalà [a,*]

[a] Department of Drug Sciences, University of Catania, V.le A. Doria 6, 95125 – Catania, Italy

[b] Department of Analytics, Environmental & Forensics, King's College London, Stamford Street, London SE1 9NH, UK

Corresponding author:

*Valeria Pittalà vpittala@unict.it

Highlights

- HO-2 selective inhibitors have been designed
- Selectivity switch from HO-1 to HO-2 was obtained by increasing the volume of the molecules
- Docking studies rationalized the obtained results
- The presence of a Tyr187 residue in HO-2 accounts for the binding pose of **9**